



Article

# Comparative Proteomic Analysis Identifies EphA2 as a Specific Cell Surface Marker for Wharton's Jelly-Derived Mesenchymal Stem Cells

Ashraf Al Madhoun <sup>1,2,\*</sup> , Sulaiman K. Marafie <sup>3</sup> , Dania Haddad <sup>2</sup>, Motasem Melhem <sup>2</sup>, Mohamed Abu-Farha <sup>3</sup> , Hamad Ali <sup>2,4</sup> , Sardar Sindhu <sup>1</sup> , Maher Atari <sup>5</sup> and Fahd Al-Mulla <sup>2</sup>

<sup>1</sup> Department of Animal and Imaging Core Facilities, Dasman Diabetes Institute, Dasman 15462, Kuwait; Sardar.Sindhu@dasmaninstitute.org

<sup>2</sup> Department of Genetics and Bioinformatics, Dasman Diabetes Institute, Dasman 15462, Kuwait; dania.haddad@dasmaninstitute.org (D.H.); motasem.melhem@dasmaninstitute.org (M.M.); hamad.ali@dasmaninstitute.org (H.A.); fahd.almulla@dasmaninstitute.org (F.A.-M.)

<sup>3</sup> Department of Biochemistry and Molecular Biology, Dasman Diabetes Institute, Dasman 15462, Kuwait; sulaiman.marafie@dasmaninstitute.org (S.K.M.); mohamed.abufarha@dasmaninstitute.org (M.A.-F.)

<sup>4</sup> Department of Medical Laboratory Sciences, Faculty of Allied Health Sciences, Health Sciences Center (HSC), Kuwait University, Jabriya 046302, Kuwait

<sup>5</sup> Medical-Surgical Pathology Department, Regenerative Medicine Research Institute, Universitat Internacional de Catalunya, 08195 Barcelona, Spain; matari@biointelligentsl.com

\* Correspondence: ashraf.madhoun@dasmaninstitute.org

Received: 28 June 2020; Accepted: 1 September 2020; Published: 3 September 2020



**Abstract:** Wharton's jelly-derived mesenchymal stem cells (WJ-MSCs) are a valuable tool in stem cell research due to their high proliferation rate, multi-lineage differentiation potential, and immunotolerance properties. However, fibroblast impurity during WJ-MSCs isolation is unavoidable because of morphological similarities and shared surface markers. Here, a proteomic approach was employed to identify specific proteins differentially expressed by WJ-MSCs in comparison to those by neonatal foreskin and adult skin fibroblasts (NFFs and ASFs, respectively). Mass spectrometry analysis identified 454 proteins with a transmembrane domain. These proteins were then compared across the different cell-lines and categorized based on their cellular localizations, biological processes, and molecular functions. The expression patterns of a selected set of proteins were further confirmed by quantitative reverse transcription polymerase chain reaction (qRT-PCR), Western blotting, and immunofluorescence assays. As anticipated, most of the studied proteins had common expression patterns. However, EphA2, SLC25A4, and SOD2 were predominantly expressed by WJ-MSCs, while CDH2 and Talin2 were specific to NFFs and ASFs, respectively. Here, EphA2 was established as a potential surface-specific marker to distinguish WJ-MSCs from fibroblasts and for prospective use to prepare pure primary cultures of WJ-MSCs. Additionally, CDH2 could be used for a negative-selection isolation/depletion method to remove neonatal fibroblasts contaminating preparations of WJ-MSCs.

**Keywords:** adult skin fibroblasts; mass spectrometry; neonate foreskin fibroblasts; proteomic analysis; Wharton's jelly-derived mesenchymal stem cells

## 1. Introduction

Mesenchymal stem cells (MSCs) are a population of non-hematopoietic stem cells with multipotent properties that are not associated with teratoma formation [1,2]. Because of these properties, MSCs are

an attractive alternative to embryonic stem cells for research and prospective clinical applications. The therapeutic potential of MSCs is not limited to their capacity to replace injured tissue cells. They also have a paracrine effect on the surrounding environment that modulates inflammation, reduces stress-induced apoptosis, and enhances revascularization [3]. MSCs have been isolated from various tissues of the human body [4–6], the bone marrow (BM) and adipose tissue (AT) are the main source for prospective clinical applications [7].

There are a number of limitations to the use of adult MSCs. For example, the procedure for the collection of BM-derived MSCs (BM-MSCs), which account for a small fraction of nucleated BM cells, is particularly invasive and restricted to the availability of suitable donors [8]. In addition, BM-MSCs have limited long-term proliferation and the differentiation potential is linked to the donor's age [9]. On the other hand, AT-derived MSCs (AT-MSCs) are more abundant and the isolation procedure is less invasive. However, the expansion and differentiation of AT-MSCs are dependent on the age and health status of the donor [10]. Wharton's jelly-derived MSCs (WJ-MSCs) continue to gain the interest of researchers as a promising alternative source of multipotent cells that do not require an invasive isolation procedure [11]. This unique population of cells is embedded within the gelatinous material of the umbilical cord, known as Wharton's jelly [12,13]. Resembling adult MSCs, WJ-MSCs have the capacity of self-renewal and immuno-modular properties [1,14–16]. As multipotent cells, WJ-MSCs can be differentiated *in vitro* into a wide spectrum of cell types from the three germ layers or at least in part, express specific markers [17–20]. Indeed, current data are conflicting in regard to the ability of MSCs to generate terminal and functional cells from either germ layer due to the use of various isolation, proliferation, and differentiation protocols that are biased due to differences in the stimulus used to induce cell signaling [21–24] in addition to the existence of cell populations at different developmental stages.

Like MSCs, WJ-MSCs are not associated with teratoma formation upon transplantation, thus clinical applications of these cells are ethically accepted [25,26]. In fact, BM-MSCs and WJ-MSCs are believed to have a common ancestor. Nevertheless, we and others have shown differences in the differentiation potential as well as the transcriptomic and proteomic profiles [1,27,28].

MSCs are often employed in the field of regenerative medicine due to their immunomodulatory effects, which virtually erases the risk of immunorejection and eliminates the need for immunosuppressive therapy prior to transplantation [29,30]. The immunomodulatory capacity of MSCs is mediated through a cell contact-dependent mechanism and the secretion of paracrine factors [31–33]. Thus, crosstalk between MSCs and immune cells is sufficient to generate a homeostatic mechanism by which MSCs regulate the immune response. Although, MSCs from different sources have comparable influences on the immunophenotype [34,35], some minor differences exist. Relative to BM-MSCs, AT-MSCs reportedly have greater immunomodulatory potency due to high levels of cytokine secretion [36] and prevention of immunogenicity [35]. On the other hand, a recent report indicated that BM-MSCs possess higher immunomodulatory activities and secrete lower amounts of paracrine signaling molecules relative to AT-MSCs and WJ-MSCs [37]. These discrepancies have been attributed to differences in cultural conditions, variations in experimental setups, and, most importantly, the crosstalk between each type of MSCs and the targeted immune cell population [38]. Although further in-depth studies are needed to clarify the immunomodulatory effects of MSCs from different sources, the advantages of perinatal vs. adult MECs include the short prenatal lifespan, limited exposure to pro-aging factors, and less cellular/genetic damage that might affect cellular plasticity [39,40].

Fibroblasts, which are the most common somatic cell type, form structural frameworks and produce an extracellular matrix that supports the surrounding tissues. Fibroblasts are not terminally differentiated cells, but rather respond to stimuli that activate proliferation and differentiation potential, and also play important roles in wound healing, inflammation, angiogenesis, and tissue fibrosis [41]. Current methods for the isolation of MSC and WJ-MSC do not prevent fibroblast contamination, as these cell populations share a spindle-like morphology, expression of common surface antigens,

and plastic adherence properties [42]. In addition to reducing the yield of these multipotent cell populations, fibroblast contamination may increase the risk of damage to MSCs and WJ-MSCs, resulting in senescence or cell death, reduced differentiation potential, or even tumorigenic transformation following transplantation [2,42].

Currently, there is no consensus on a single surface marker to differentiate WJ-MSCs from fibroblasts of various sources, which is essential for the isolation of pure and authentic populations of WJ-MSCs that can be introduced into damaged tissues or organs without passaging in tissue culture, for prospective clinical applications. In this study, the proteomic profiles of membrane-bound proteins extracted from WJ-MSCs, neonatal foreskin fibroblasts (NFFs), and adult skin fibroblasts (ASFs) were characterized using nanoscale liquid chromatography coupled to tandem mass spectrometry (Nano LC-MS/MS). Gene expression analysis at the transcriptional and protein levels indicated that ephrin type-A receptor 2 (EphA2) is a candidate surface-specific protein for the identification of WJ-MSCs, whereas cluster of differentiation (CD)H2 and Talin2 are markers for NFFs and ASFs, respectively.

## 2. Results

### 2.1. Analysis of Differentially Expressed Proteins Detected by Nano LC-MS/MS

To illustrate differences in the proteomic patterns between different passages of WJ-MSCs, ASFs, and NFFs, membrane-fraction protein extracts were digested, and the generated peptides were detected by Nano LC-MS/MS. Although there were some variations in the number of proteins identified between passages, most proteins were common among different passages of the same cell type. In total, 958, 866, and 813 proteins were shared among the different passages of WJ-MSCs, ASFs, and NFFs, respectively (Figure 1A). Then, we compared the number of proteins shared among different cell-types and identified 905 proteins that were commonly expressed among WJ-MSCs, ASFs, and NFFs (Figure 1B). Among the cell types, a total of 97 differentially expressed proteins were identified, including 56 that were unique to WJ-MSCs, 23 unique to NFFs, and 18 unique to ASFs. Moreover, 41 proteins were shared between WJ-MSCs and NFFs, 60 between WJ-MSCs and ASFs, and 23 between ASFs and NFFs.

The identified proteins were first screened to identify all membrane-bound proteins that could be potential candidate cell surface markers. Of the initial 1126 screened proteins, 454 were found to have a transmembrane domain, and then categorized according to involvement in biological processes, molecular functions, and cellular localization using gene ontology (GO) enrichment methods (Figure 2). Of the proteins involved in biological processes, most had intracellular transport functions or targeted the cellular membranes and organelles. Several proteins were associated with RNA processing, cell biogenesis, and organization (Figure 2A). Of the proteins involved in molecular functions, most were either associated with RNA binding functions, cell signaling, or the ribosomal complex (Figure 2B). Most of the detected proteins were present in vesicles, membrane-bound organelles, or secretory exosomes (Figure 2C).

Quantitative MS was performed to identify proteins with differential expression patterns in different cell types. These proteins were compared and classified based on their cellular localization, as well as involvement in biological processes and molecular functions (Tables 1 and 2). Many of the identified proteins were common among different cell types, while others were specific to a particular cell type. For example, proteins involved in plasma membrane rafts and cell–cell junctions were specific to a particular cell type, including EphA2 in WJ-MSCs, the cytoskeletal anchoring protein Talin2 (TLN2) in ASFs, and neuronal (N)-cadherin (CDH2/CD325) in NFFs (Table 1, Cytoplasmic membrane). In the mitochondria, the adenosine di/triphosphate (ADP/ATP) translocase 1/solute carrier family 25 member 4 (SLC25A4) and voltage-dependent anion-selective channel protein VDAC3 appear to be specific to WJ-MSCs, while mitochondrial superoxide dismutase (SOD2) was identified in both WJ-MSCs and ASFs. The integrin alpha subunit ITGA2 (CD49b) was common to both WJ-MSCs and NFFs, while lipase maturation factor (LMF2) was detected specific to fibroblasts (both ASFs and NFFs).

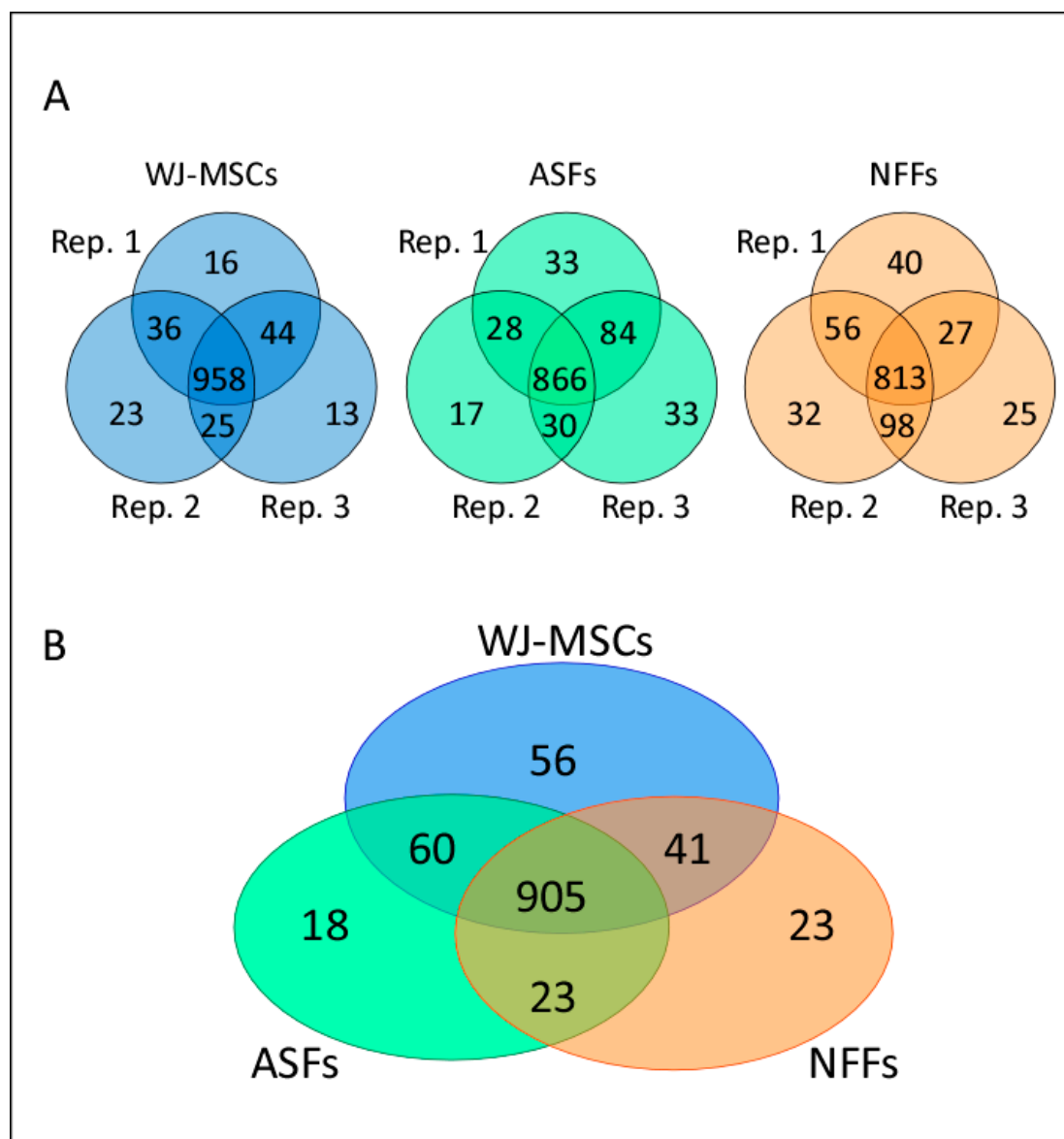


**Figure 1.** Proteomic analysis of WJ-MSCs, ASFs and NFFs. **(A)** A Venn diagram illustrating the number of proteins expressed by three different cell passages of WJ-MSCs, ASFs, and NFFs. For each cell type, the overlapping areas between the cell passage populations indicate the numbers of commonly expressed proteins. **(B)** A Venn diagram showing the number of proteins expressed by each cell type. The overlapping areas indicate the numbers of proteins commonly expressed by WJ-MSCs, ASFs, and NFFs, as identified by MS analysis. Rep, replicate.

In addition, the dataset contains shared and cell type-specific proteins within many functional classes, thereby revealing important differences in the protein profiles of specific cell types (Table 2). For example, signaling proteins known to be involved in the tricarboxylic acid cycle were detected in all of the cell types studied. On the other hand, the notch signaling protein ANXA4 was specific to fibroblasts. The Wnt signaling molecules CTHRC1 and CDH2 were only detected in WJ-MSCs and NFFs respectively, whereas Ras homolog family member A (RHOA) and ubiquitin A-52 residue ribosomal protein fusion product 1 (UBA52) were present in both WJ-MSCs and ASFs. Similarly, the studied cell types had notable differentially expressed proteins involved in other biological mechanisms, including metabolic and oxidation-reduction, cell adherence, cell component transportation, and biogenesis (Table 2). Thus, the proteomic dataset provides an important resource of cell-surface proteins present on WJ-MSCs that could be used in future functional studies.

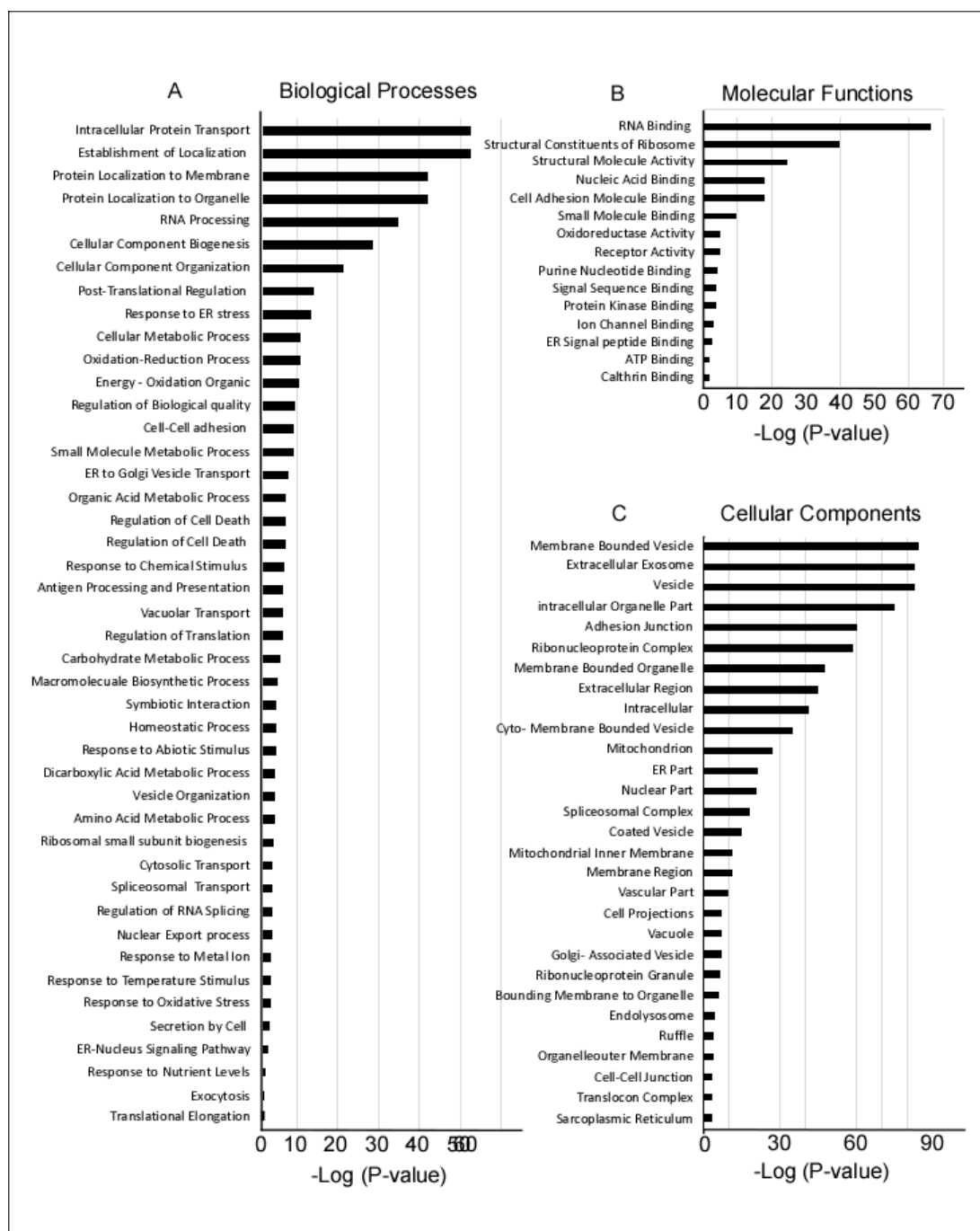


**Figure 2.** Pathways and gene ontology (GO) enrichment analysis of 1126 proteins expressed by WJ-MSCs, ASFs, and NFFs. The GO annotation enrichment score [ $-\text{Log}_2(p\text{-value})$ ] analysis of proteins involved in biological processes (A), molecular functions (B), and cellular components (C), as identified by MS and in proteomic analysis.

**Table 1.** Cellular localization of the membrane-bound proteins differentially expressed by WJ-MSCs, ASFs, and NFFs. – means un-detected.

Cellular Localization	Unique to WJ-MSCs	Unique to NFFs	Unique to ASFs	WJ-MSCs and NFFs	WJ-MSCs and ASFs	ASFs and NFFs
Extracellular Exosome	ANP32B, ALDH1A3, ATP1B3, ATP2B1, DDX19B, DYNC2H1, EIF3E, GRHPR, HSPA2, ICAM1, NUCB2, PFKL, PFDN2, PDCD5, PCMT1, RAB5A, TMEM106B, TUBB3, VDAC3	CDH2, EFHD1, RAB3B, RAB3B, SNRPE, TPP1	AK1, ATP6V1A, GNAL, NDRG1, QDPR, SIRPA, TUBB4A, UBE2V2	COLEC12, DSTN, DLST, ECHS1, IGF2R, IGF2R, IGF2R, IDH1, IDH2, NDUFB4, PRDX3, PLD3, REEP5, SCAMP3, STX12, TMED9, TPM3, USP14	ADH5, CAPN1, CAPN2, DNAJB4, EMILIN1, GLIPR2, GFPT1, ITSN2, LTA4H, HLA-B, HLA-C, MARS, PDLIM2, PEPD, PSMC6, PSMB6, RHOA, RHOC, RAC1, RAC2, RAC3, RNH1, RPS17, STK10, SOD2, TXNL1, TIMP3, FLJ44635, TCEB2, TPT1, UBE2L3	ANXA4, CYB5A, GNB2, GNB4, LAMTOR1, PCK2, PTGS1, PRKCA, RPLP1, SNX18
Cell–Cell Adhesion	DDX6, EPHA2, GCN1, LIMS1, BZW2, PCMT1	CDH2, GOLGA3, STAT1, TMOD3	TLN2	IDH1, KTN1, MACF1	EFHD2, SWAP70, MYH9, PSMB6, RHOA, TJP2, TWF1	OXTR, SNX1
Cellular Adherence	DDX6, ICAM1, LIMS1, TGFB11I	STAT1	TNS3	DPP4, IGF2R, ITGA2, IDH1	CAPN2, RAC1, TLN2	CAPN1
Mitochondria	C1QBP, LETM1, PYCR1, PYCR2, SLC25A4, SQRDL, VDAC3	EFHD1	–	BRI3BP, NDUFB4, DLST, ECHS1, IDH2, PRDX3, PITRM1	ALDH18A1, DLD, GLUD1, OGDH, SOD2	CYB5A, PCK2, PRKCA
Mitochondrial Envelope	LETM1, SLC25A4, SQRDL, VDAC3	EFHD1, SLC25A1	–	NDUFB4	ALDH18A1, OGDH, SOD2	CYB5A, COX1, PRKCA
Endoplasmic Reticulum (ER)	APOL2	MLEC, PML	–	PLD3, REEP5, TMED9	CAPN2, HLA-B, HLA-C, RHOA, RAC1, SEC24D	CYB5A, LMF2, PTGS1
ER Membrane	APOL2	RAB2B	–	KTN1	HLA-B, HLA-C, RAC1, SEC24D	CYB5A, PTGS1
Nuclear Parts	C1QBP, DDX6, LSM2, NUP93, TGFB11I, WDR36	STAT1, SNRPE, SART3, TPP1	–	ADAR, DLST, ECHS1, IGF2R, IDH1, NDUFB4, PITRM1, SPARC, TP53BP1, U2AF1	GLUD1, OGDH, PPP3CA, SRRT, SF1, SOD2, TCEB2	PRKCA
Plasma Membrane Raft	EPHA2, RAB5A	CDH2	TLN2	ATP1B3, MACF1, TPM1	PRKAR1A, RAC1, TWF1	–
Cytoplasm Membrane		RAB3B, TPP1	PACS1	ATP1B3, DPP4, IGF2R, SPARC, STX12, USP14	HLA-B, HLA-C, RAC1, SEC24D	AP1B1
Intracellular Membranes	APOL2, C1QBP, DDX19A, DDX19B, DDX6, LETM1, LIMS1, LSM2, NUCB2, NUP93, PFKL, SLC25A4, SQRDL, TGFB11I, VDAC3	EFHD1, RAB2B, RAB3B, STAT1, SNRPE, SLC25A1, SART3, TPP1	PACS1, RANBP2, RGPD3, RGPD4, RGPD5, RGPD6, RGPD8, TNS3	ADAR, ATP1B3, DLST, DPP4, ECHS1, IGF2R, ITGA2, IDH1, KTN1, NDUFB4, PITRM1, SCRNI, SPARC, STX12, TPM2, TP53BP1, U2AF1, USP14	ALDH18A1, CAPN1, CAPN2, GLUD1, GLUD2, HLA-B, HLA-C, OGDH, PRKAR1A, PPP3CA, RAC1, SEC24D, STRAP, SRRT, SF1, SOD2, TLN2, TCEB2, TPM3	AP1B1, COX1, PGP, PTGS1, PRKCA, RPLP1, ADH5
Spliceosome	LSM2	SNRPE	–	ADAR	SNRPA, SF1	–

WJ-MSCs, Wharton’s jelly-derived mesenchymal stem cells; ASFs, Adult skin fibroblasts; NFFs, Neonate foreskin fibroblasts.

**Table 2.** Involvement of the identified membrane-bound proteins in signal transduction pathways and biological processes that were differentially by WJ-MSCs, ASFs, and NFFs. – means un-detected.

Signaling Pathways	Unique to WJ-MSCs	Unique to NFFs	Unique to ASFs	WJ-MSCs and NFFs	WJ-MSCs and ASFs	ASFs and NFFs
Signal Transduction Pathway						
Wnt	CTHRC1	CDH2	–	–	RHOA, UBA52	–
NF-κB	–	–	–	–	PSMB6	–
Notch	–	–	–	–	–	ANXA4
Interferon	–	–	–	ADAR, STAT1	HLA-B, HLA-C	–
Insulin/Glucose	NUP93, PFKL	–	ATP6V1A, RANBP2	–	–	–
Amino Acid Biosynthesis	PYCR1, PYCR2	–	–	–	ALDH18, GLUD1	–
Tricarboxylic Acid Cycle	–	–	–	DLST, IDH1, IDH2,	DLD, OGDH	–
Intracellular Transport	DDX19A, DDX19B, NUP93, RPL9	SNRPE	RANBP2, RGPD3, RGPD4, RGPD5, RGPD6, RGPD8	ADAR, STX12, U2AF1	PPP3CA, RPS17, SEC24D	AP1B1, RPLP1
RNA Processing	C1QBP, LSM2, RPL9, WDR36	SNRPE, SART3	–	ADAR, RPS17, U2AF1	STRAP, SRRT, SNRPA, SF1	RPLP1
Cell Component Biogenesis	DDX6, LIMS1, WDR36, C1QBP, ICAM1, NUP93, PFKL, VDAC3	SNRPE, SART3	–	NDUFB4, ADAR, ITGA2, STX12	SEC24D, PRKAR1A, RAC1, STRAP, SF1, SOD2, TLN2, TCEB2	PRKCA, RPLP1
Oxidation-reduction Process	NUCB2, PFKL, SQRDL	–	–	NDUFB4, DLST, ECHS1, IDH	CYB5A, COX1, PTGS1ADH5, ALDH18A1, GLUD1, GLUD2, OGDH, SOD2	–
Cell Adhesion	C1QBP, DDX6, ICAM1, TGFB11	STAT1	–	DPP4, ITGA2, IDH1, KTN1	PRKAR1A, PPP3CA, RAC1	PRKCA
Metabolic Processing	APOL2, NUCB2, PFKL	SLC25A1	RANBP2	DLST, ECHS1, IDH1, NDUFB4	ADH5, ALDH18A1, GLUD1, GLUD2, OGDH	CYB5A, COX1, PGP, PTGS1, PRKCA
Post-Translational Modifications	C1QBP, DDX6	–	–	ADAR	SRRT	PRKCA

WJ-MSCs, Wharton's jelly-derived mesenchymal stem cells; ASFs, Adult skin fibroblasts; NFFs, Neonate foreskin fibroblasts.

## 2.2. Quantitative RT-PCR Analysis of Gene Products (Proteins) Identified by Mass Spectrometry (MS) Screening

While generally a good indicator of protein translation in the cells, the mRNA level is not always correlated with the presence of the encoded protein [43]. Thus, to verify whether the relative expression levels of the proteins detected via MS in different cell types could have been predicted by the mRNA levels; quantitative reverse transcription polymerase chain reaction (qRT-PCR) analysis was performed to analyze the gene expression (Figure 3). The expression pattern of CD73, a well-known marker of WJ-MSCs was also analyzed, which showed comparable expression levels in both WJ-MSCs and fibroblasts (Figure 3).

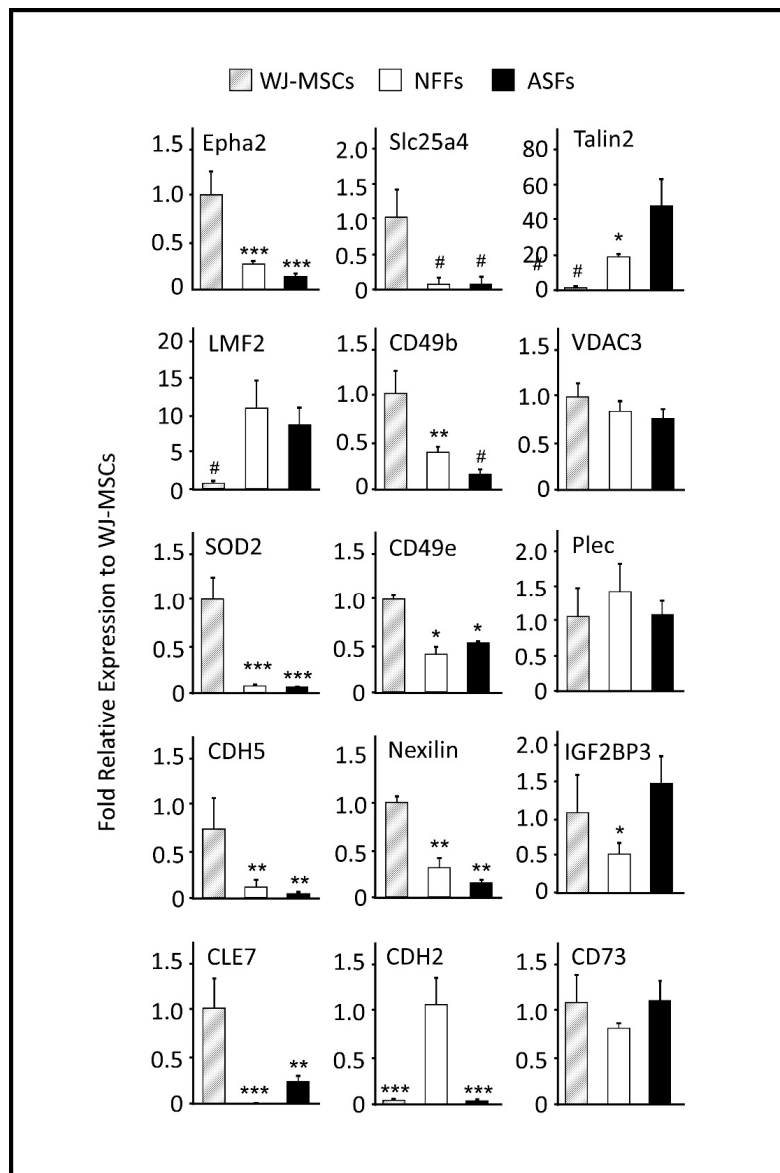


**Figure 3.** qRT-PCR analysis of 15 selected genes differentially expressed by WJ-MSCs, ASFs, and NFFs. Relative quantification was calculated by comparing gene expression levels in ASFs and NFFs with corresponding WJ-MSCs expression, which was set to 1 (control sample). Gene expression was initially normalized to the geometric mean for the housekeeping genes  $\beta$ -actin, Glyceraldehyde 3-phosphate dehydrogenase (GAPDH), and S18, as references. Data are presented as the means  $\pm$  standard deviation of six qRT-PCR assays (technical duplicate of three biological samples). \*  $p < 0.05$ , \*\*  $p < 0.01$ , and \*\*\*  $p < 0.001$  are significant to the higher bar. #  $p < 0.01$  is significant to all other bars.

The mRNA expression profiles of the membrane-bound proteins EphA2, SLC25A4, TLN2, LMF2, and CD49b were similar by qRT-PCR analysis and the quantitative MS spectra. EphA2 and SLC25A4 were predominantly expressed by WJ-MSCs. The expression levels of EphA2 in ASFs and NFFs were only 13% and 27% relative to those of WJ-MSCs, respectively. While SLC25A4 transcripts in both fibroblast cell types were <10% relative to those of WJ-MSCs. On the other hand, TLN2 and LMF2 genes were notably expressed by fibroblasts. In both ASFs and NFFs, the expression levels of TLN2 and LMF2 were 43- and 12-fold, and 17- and 15-fold relative to that of WJ-MSCs, respectively (Figure 3). CD49b was expressed mainly by WJ-MSCs, to a lesser extent by NFFs (40% to that of WJ-MSCs), and as low as 15% in ASFs. Alternatively, mRNA levels of VDAC3, SOD2, and plectin-1 (PLEC1) did not reflect the associated protein expression levels determined by MS analysis (Table 3), whereas SOD2 expression levels were 20-fold higher in WJ-MSCs than fibroblasts. The mRNA expression levels of VDAC3 and PLEC1 were equivalent in all cell types (Figure 3).

**Table 3.** Protein levels predicted by MS analysis, mRNA expression by real time quantitative reverse transcription polymerase chain reaction (qRT-PCR), and protein levels detected by Western blot analysis. – means un-detected; + means detected.

Gene Symbol	Protein Name	Protein Expression Levels Determined by MS			mRNA Levels Determined by qRT-PCR			Protein Levels Determined by Western Blot		
		WJ-MSCs	NFFs	ASFs	WJ-MSCs	NFFs	ASFs	WJ-MSCs	NFFs	ASFs
<i>EPHA2</i>	EPH receptor A2	+	–	–	+++	+	–	+++	+	+
<i>SLC25A4</i>	ADP/ATP translocase 1	+	–	–	++	–	–	+++	–	–
<i>TLN2</i>	Talin2	+	–	+	–	+	+++	–	–	+++
<i>LMF2</i>	Lipase maturation factor 2	–	+	+	–	++	++	+	+	++
<i>ITGA2</i>	CD49b/Integrin subunit alpha 2	+	+	–	++	+	–	+++	++	–
<i>VDAC3</i>	Voltage-dependent anion channel 3	+	–	–	+	+	+	+++	+	+++
<i>SOD2</i>	Superoxide desmutase	+	–	+	+	–	–	+++	–	–
<i>CDH2</i>	CD325/N-Cadherin	–	+	–	–	+++	–	–	–	–
<i>ITGA5</i>	CD49e/Integrin subunit alpha 5	++	+	+	++	+	+	++	+	+
<i>IGF2BP3</i>	Insulin-like growth factor 2 mRNA binding protein 3	–	–	+	++	+	++	–	–	–
<i>PLEC</i>	Plectin	–	+	+	+	+	+	++	++	++
<i>CLE7</i>	RNA transcription, translation and transport factor	+	–	–	+	–	–	+++	+	+
<i>CDH5</i>	CD144/VE-cadherin	–	–	–	++	+	–	++	+	+
<i>NEXN</i>	Nexilin	+	–	–	++	+	–	+	+	+
<i>MLCK1</i>	Myosin light chain kinase	+	–	–	–	–	–	–	–	–

The expression levels of the integrin subunit integrin alpha-5 (ITGA5, CD49e), insulin-like growth factor 2 mRNA-binding protein 3 (IGF2BP3), the RNA transcription, translation and transport factor CLE7, the vascular-endothelial VE-cadherins (CDH5, CD144), and the actin-binding protein Nexilin were also analyzed. The mRNA quantifications by qRT-PCR results revealed that CD49e, CLE7, CDH5, and Nexilin were primarily expressed by WJ-MSCs. In fibroblasts, CD49e transcripts were 50% lower than in WJ-MSCs, while CLE7 transcripts were absent in NFFs and accounted for less than 24% in ASFs relative to WJ-MSCs (Figure 3). CDH5 and Nexilin mRNAs were >4- and >6-fold higher than in WJ-MSCs fibroblasts, respectively (Figure 3). On the other hand, IGF2BP3 was expressed mostly in WJ-MSCs and ASFs, while CDH2 transcripts were predominately expressed by NFFs (>80-fold vs. other cell-types, Figure 3).

### 2.3. Western Blot Analysis

Western blot analysis of selected proteins was performed to validate the quantitative proteomic results obtained by MS and to assess correlations with the mRNA levels determined by qRT-PCR (Figure 4). As compared to the findings of MS and qRT-PCR, the protein levels of CD49b, as determined by Western blot analysis, were approximately 8-fold higher in WJ-MSCs and NFFs relative to ASFs. On the other hand, levels of mitochondrial SOD2 were higher in WJ-MSCs, in agreement with their mRNA levels, but were not detected in ASFs, as predicted by the proteomics approach (Table 3). Western blot analysis using specific antibodies barely detected SOD2 proteins in fibroblasts (Figure 4). Protein levels of PLEC1, Nexilin, TLN2, and CD49e replicated the expression patterns determined by qRT-PCR analysis. However, the expression levels of these proteins in different cell types did not

mimic those predicted by the proteomics approach. PLEC1 and Nexilin proteins were comparably expressed by all cell types, whereas CD49e proteins were equivalently detected in WJ-MSCs and ASFs but were 50% lower in NFFs. On the other hand, TLN2 was predominately observed in ASFs and seldomly detected in WJ-MSCs or NFFs. Protein levels of LMF2 were 5-fold greater in ASFs relative to WJ-MSCs, but not expressed in NFFs, as observed by both qRT-PCR analysis and the initial MS screening. Similarly, EphA2 and SLC25A4 were predominantly expressed by WJ-MSCs, as predicted by the proteomics approach and validated by qRT-PCR (accounting for <20% in fibroblasts, Figure 4 and Table 3).

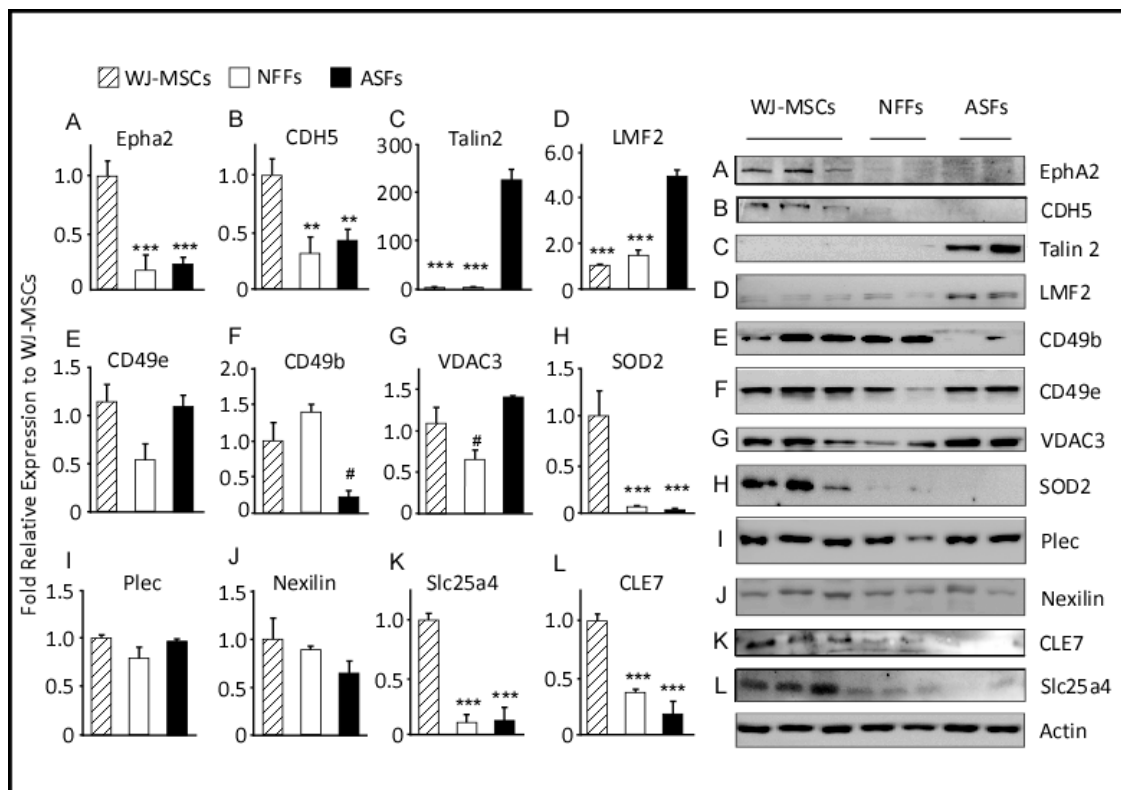


**Figure 4.** Expression levels of proteins differentially expressed by WJ-MSCs, ASFs, and NFFs. Representative Western blots of 12 expressed proteins. Normalized proteins are expressed relative to their prospective expression in WJ-MSCs. Data are presented as the means  $\pm$  standard error of the mean of three independent assays. \*\*  $p < 0.01$ , and \*\*\*  $p < 0.001$  are significant to the higher bar. #  $p < 0.01$  is significant to all other bars.

#### 2.4. Fluorescence Microscopy

Next, fluorescence microscopy was used to visualize the expression patterns and the cellular localizations of proteins of interest in WJ-MSCs, ASFs, and NFFs (Figure 5). SOD2 was detected predominantly in WJ-MSCs with lower expression seen in NFFs. CD49b was mostly expressed by WJ-MSCs, with some expression detected in ASFs. On the contrary, TLN2 was observed only in ASFs, confirming the results obtained by Western blot analysis. LMF2 was expressed mainly in ASFs, with some minor expression patterns in NFFs, correlating with the pattern detected by Western blot analysis. The myosin light chain kinase MLCK1 was expressed mostly in NFFs, with lower levels in ASFs, similar to the expression profile of N-cadherin (CD325).

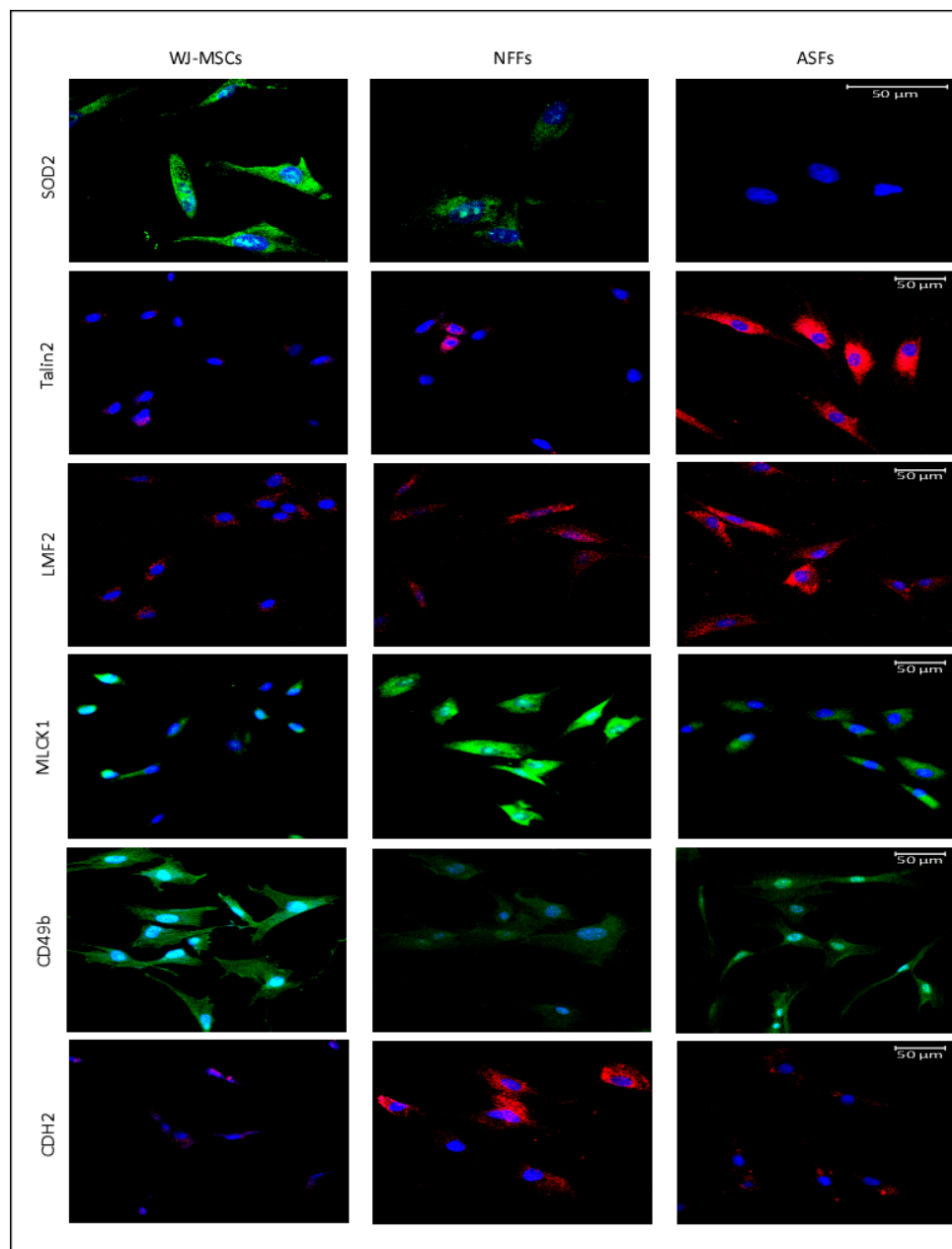


**Figure 5.** Immunofluorescence of selected proteins expressed in WJ-MSCs, NFFs, and ASFs. Representative confocal laser microscopy images of immunofluorescence for primary cells using APEX antibody labeling system for conjugating the indicated primary antibodies as described in the Materials and Methods Section. Shown at 400× magnification. Nuclei were stained with 4',6-diamidino-2-phenylindole (DAPI).

### 3. Discussion

Due to the potential use in regenerative medicine, WJ-MSCs have continued to attract the interest of academic and medical communities in recent years. Despite a multitude of studies, the isolation of WJ-MSCs from contaminating cell populations remains difficult, particularly with fibroblasts. In order to develop more convenient and targeted methods of purification, cell-specific surface markers were identified to precisely isolate WJ-MSCs.

According to the current criteria defined by the International Society for Cellular Therapy, MSCs express the membrane proteins CD105, CD73, and CD90, but not CD45, CD34, CD14, or CD11b, CD79 $\alpha$ , or CD19, and HLA-DR [11]. Besides the present study, several previous studies have reported that

many of these surface markers are shared with fibroblasts [2,11,42,44–47]. On the other hand, MSCs express various fibroblast proteins, such as collagen, vimentin, fibroblast surface protein, heat shock protein 47, and  $\alpha$ -smooth muscle actin [2,44]. Thus, MSCs are a heterogeneous cell population that lacks a specific surface biomarker, thereby rendering identification and characterization of MSCs rather challenging. In this study, 454 membrane-bound proteins differentially expressed by these cell types were identified. Here, a few highly expressed markers were selected for further analysis, which included EphA2, CDH5, and the integrin alpha subunits CD49b and CD49e.

EphA2 belongs to the Ephrin receptor subfamily of the protein-tyrosine kinase family. EphA2 and its ligand Ephrin play important roles in cellular migration, survival, and differentiation [48]. In general, Ephrin receptors mediate cell-to-cell binding, leading to contact-dependent bidirectional signaling to neighboring cells [49]. During embryogenesis, Ephrin receptors mediate neuron differentiation, neural-tube formation, and development of the early hindbrain [50]. Ephrin receptors influence a niche of stem cells. In the present study, EphA2 was primarily expressed by WJ-MSCs supporting its role in cell self-renewal and differentiation [51]: the two major characteristics of stem cells that fibroblasts lack. The results of previous gene expression studies indicate that MSCs derived from BM and AT express a wide range of Ephrin receptors, including EphA2 [48], whereas MSCs isolated from the umbilical cord blood expresses EphB2 [52]. In support of our data, proteomic analysis identified EphA2 as a marker of MSCs derived from the placenta, a cell type that is developmentally related to WJ-MSCs [53] and is believed to secrete prostaglandin E2, an anti-fibrosis and immunomodulator marker [54]. Together, these data indicate that EphA2 is an important surface marker of WJ-MSCs.

CDH5 or VE-cadherin have been previously described to be a surface marker for Adult cardiac progenitor/stem cells but not BM-MSCs [55] or WJ-MSC [56], here we found it to be a good surface marker for WJ-MSCs and to a lesser extent to NFFs. CDH5 is a calcium-dependent cell adhesion protein that ensure integrity of blood and lymph vessels and play an important role in vasculogenesis, angiogenesis, vessel leakage, and leukocyte trafficking [57]. Inhibition of CDH5 expression, by miRNA-6086, blocks human embryonic stem cells' differentiation into endothelial cells [58]. Together, the elevated levels of CDH5 in WJ-MSCs supports their prospective differentiation into endothelial cells or possible other lineages.

Integrins play an essential role in cellular adhesion and cell surface-mediated signaling. CD49b is integrin alpha 2 subunit, which, in combination with integrin beta 1 subunit, forms a receptor for collagen, collagen C-propeptides, fibronectin, laminin, and E-cadherin [59]. Ligand recognition and binding occur mainly through the alpha subunit of the integrin heterodimer. Once activated, the receptor initiates downstream signaling events engendering changes in cell migration, survival, and growth [60]. Interestingly, integrin activation via intracellular ligands has also been reported. The binding of Talin 2 to the integrin beta subunit leads to a conformational change to its transmembrane domain, leading to integrin activation [61].

Albeit BM-MSCs and fibroblasts express similar levels of CD49b [62]; in the present study, mRNA and protein expression levels of CD49b were 2.5-fold higher in WJ-MSCs than in NFFs. This pattern is corroborated by two large transcriptomic and proteomic studies [63,64], which were generated the Human Protein Atlas (HPA). In the HPA, CD49b is mostly expressed by endothelial cells derived from the umbilical vein and to a lower extent in NFFs. The mRNA and protein expression patterns of CD49e observed in this study also mimicked those from the HPA database: mostly expressed by endothelial cells from the umbilical vein and lower expression in NFFs [59].

While several studies have screened and identified surface markers of MSCs, the identification of MSC-specific surface markers remains challenging. A systematic review of available information noted a great discrepancy in the expression patterns of several surface markers of MSCs in different studies [65]. A possible explanation for this discrepancy is related to the origin or heterogeneity of the MSCs used in different studies. Alternatively, these differences could possibly be related to the different proliferative stages of the cells in culture. In any case, further studies are needed to validate our preliminary findings as well as extrapolate the findings of previous studies to overcome inconsistencies

regarding cell surface marker profiles of MSCs with the potential advantage of culture purification of WJ-MSCs via negative or positive selection. A limitation to this study is the comparison of data with only two fibroblast cell lines. Hence, the results must be interpreted with caution.

To the best of our knowledge, this is the first study that aimed to identify specific cell markers for WJ-MSCs that are not present in fibroblasts of neonate or adult origin. We confirmed EphA2 as a potential cell surface marker that distinguishes WJ-MSCs from fibroblasts and can be used to prepare pure WJ-MSCs primary cell cultures. CDH5 or VE-Cadherin can be also used as a surface marker, however it would yield a less pure WJ-MSCs population. Whereas, a negative-selection isolation process can be devised using CDH2 to remove neonatal fibroblasts, commonly encountered in WJ-MSCs preparations. Currently, we are aiming to use these surface-specific markers to prepare pure cell cultures from a wide range of MSCs derived from several tissues, including bone marrow, adipose tissue, and dental pulp.

#### 4. Materials and Methods

##### 4.1. Ethical Permission and Procurement of Human Samples

The study protocol approved by the Ethical Review Committee of the Dasman Diabetes Institute (protocol No: 2013-009) and conducted in accordance with the World Medical Association Declaration of Helsinki—Ethical Principles for Medical Research Involving Human Subjects. Human WJ-MSCs, NFFs, and ASFs were purchased from the ATCC (PCS-500-010, CRL-2522, and PCS-201-012, respectively).

##### 4.2. Culture and Maintenance of WJ-MSCs, NFFs, and ASFs

WJ-MSCs were cultured in Dulbecco's modified Eagle's medium (DMEM)/Hams' F12 medium (1:1 v/v; Invitrogen Corporation, Carlsbad, CA, USA) supplemented with 15% MSC-qualified fetal bovine serum (FBS; Invitrogen Corporation) and 100 U/mL of penicillin-streptomycin (Gibco, Carlsbad, CA, USA). WJ-MSCs (passage 2) were cultured at approximate densities of 300–1000 cells/cm<sup>2</sup> in 100 mm plates to generate colony-forming units. After 7–10 days, the culture medium was removed, cells were washed with 1× phosphate buffer saline (PBS), and cell colonies were transferred into individual 100 mm plates for expansion. NFFs and ASFs were cultured in DMEM supplemented with 10% FBS and 100 U/mL of penicillin-streptomycin. At 60% confluency, cell cultures were harvested for passaging and/or scraped for protein isolation, RNA extraction, or immunofluorescence analysis.

##### 4.3. Preparation of Protein Extract for MS Analysis

Three replicates from three different passages (between passage 2 and 5) for each cell type (WJ-MSCs, NFFs, or ASFs) were used for the proteomic analysis. The cells were washed with cold PBS, lysed in 500 µL of lysis buffer (6 M urea, 4% CHAPS hydrate) supplemented with a mini complete protease inhibitor cocktail (Roche Diagnostics, Laval, QC, Canada) for 30 min at 4 °C, and then homogenized. Following centrifugation at 14,000 rpm for 30 min at 4 °C, protein concentrations were determined by Bradford method using γ-globulin as a standard, and proteins were subjected to centrifugal proteomic reactor as described previously [66]. Briefly, 20 µg of total proteins were mixed with 10 µL of a strong cationic exchange BcMag™ SCX Magnetic bead slurry (Bioclone, San Diego, CA, USA) and vigorously vortexed in 1 mL of 5% formic acid. The mixture was centrifuged, and the pellet was resuspended in 1 mL of 0.5% formic acid. Then, 20 µL of a reducing solution (150 mM ammonium bicarbonate, 20 mM dithiothreitol) was added to the samples for 15 min at 56 °C with constant rotation. Then, 20 µL of an alkylating solution (150 mM ammonium bicarbonate, 100 mM iodoacetamide) was added for 15 min at room temperature. The alkylation reaction was stopped by the addition of 1 mL of 0.5% formic acid. The beads were centrifuged, and the proteins were digested with trypsin at 37 °C for 24 h with constant shaking. The generated peptides were eluted with 1 mL of 5% formic acid, lyophilized to complete dryness in a speed-vac, and stored at −20 °C until subjected to MS analysis.

#### 4.4. Nano Liquid Chromatography with Tandem Mass Spectrometry (LC-MS/MS) Analysis

Proteomics were analyzed using LC-MS/MS (LTQ-Orbitrap Velos; Thermo Fisher Scientific, Waltham, MA, USA) as described previously [67]. Briefly, peptides were resuspended in 5% formic acid and then loaded on a C18-A1 easy column for desalting (Proxeon Biosystems A/S, Odense, Denmark). Desalted peptides were then directed to a C18-A2 analytical easy column and eluted at a gradient of 5% to 35% acetonitrile with 0.1% formic acid for 120 min (Proxeon Biosystems A/S). Full MS scanning was performed at a resolution of 60,000 and the top 20 spectra were obtained in the data-dependent acquisition mode. Raw data files were analyzed using Maxquant 1.3.0.5 software (Thermo Fisher Scientific GmbH, Driesch, Germany) using the Sequest tandem MS data analysis program and the Mascot search engine against the *Homo sapiens* International Protein Index protein sequence database version 3.68 (European Bioinformatics Institute, Cambridge, UK), as described previously [67], with the following search parameters: the digestive enzyme trypsin, with two miss-cleavages permits, fixed modification, carbamidomethyl of cysteine, variable modification, methionine oxidation, and a false discovery rate (FDR) of 1% for peptide confidence. The identified proteins were quantified using Sieve software version 1.3 (Thermo Fisher Scientific GmbH). Ingenuity pathway analysis software (Ingenuity Systems, Inc., Redwood City, CA, USA) was used for analyses of molecular functions and protein networks.

#### 4.5. Functional Enrichment Analysis

Functional enrichment analyses were performed using the Database for Annotation, Visualization and Integrated Discovery (DAVID) functional annotation tool (<http://david.abcc.ncifcrf.gov/>). All identified proteins from different cell types with an FDR threshold of <10% and default options and human Encyclopedia of DNA Elements (ENCODE) as a background were searched according to the following annotation categories: GeneOntology cellular components (GOTERM\_CC\_FAT), molecular functions (GOTERM\_MF\_FAT), and biological processes (GOTERM\_BP\_FAT), along with Protein Analysis Through Evolutionary Relationships (PANTHER) molecular functions, biological processes and pathways, Kyoto Encyclopedia of Genes and Genomes pathways, and the InterPro and Simple Modular Architecture Research Tool (SMART) protein domains (for all analyses, a FDR threshold of 10% was applied for multiple testing). Only the following GO terms were significantly enriched in our gene list (with 446/456 genes having a DAVID gene ID): “extrinsic to membrane” (GOTERM\_CC\_FAT), “cytoskeletal protein binding,” “purine ribonucleotide binding,” and “ribonucleotide binding” (GOTERM\_MF\_FAT).

#### 4.6. Western Blot and Immunofluorescence Assays

Western blot analysis was performed as described previously [68]. Briefly, cells were harvested and lysed in modified radioimmunoprecipitation assay buffer. Cell lysates were quantified using the Pierce BCA Protein Assay Kit (Thermo Fisher Scientific) and equal amounts of protein were resolved on 8%–12% polyacrylamide gels and transferred to polyvinylidene fluoride membranes (EMD Millipore Corporation, Billerica, MA, USA). After blocking, the membranes were blotted with the corresponding primary and horseradish peroxidase-linked secondary antibodies (Supplementary Table S1). Proteins were visualized using Amersham ECL Prime Western Blotting Detection Reagent (GE Healthcare Life Sciences, Chicago, IL, USA). Images were captured using the VersaDoc™ MP 5000 imaging system (Bio-Rad Laboratories, Hercules, CA, USA).

Immunofluorescence was performed as described previously [69]. Briefly, cells were cultured overnight on glass coverslips coated with 0.1% gelatin, fixed with 4% paraformaldehyde for 15 min, permeabilized with 10% Triton X-100 for 30 min, and incubated overnight with appropriate antibodies (Supplementary Table S1). Primary antibodies were conjugated with Alexa Fluor 594 or Alexa Fluor 488 using APEX Antibody Labeling Kits (Invitrogen Corporation). Fluorescent images were captured

using a confocal laser-scanning microscope (LSM 710; Carl Zeiss AG, Oberkochen, Germany) as previously described [70].

#### 4.7. RNA Extraction, cDNA Synthesis, and qRT-PCR Reactions

Total RNA was extracted from cells using the total RNA purification kit (Norgen Biotek Corp, Thorold, ON, Canada) in accordance with the manufacturer's protocol. Total RNA was quantified using a NanoDrop 2000c spectrophotometer (Thermo Fisher Scientific) and RNA integrity was evaluated by 2% agarose gel electrophoresis (data not shown). First-strand cDNA was synthesized from 200 ng RNA by reverse transcription using the QuantiTect Reverse Transcription Kit (Qiagen Inc., Valencia, USA). The qRT-PCR reactions were performed as described elsewhere [71]. Primer pairs (Supplementary Table S2) were selected from the PrimerBank database (<https://pga.mgh.harvard.edu/primerbank/>) [72] and tested for equivalent efficiency. Quantitative polymerase chain reaction (qPCR) was performed on the ABI7900 system (Applied Biosystems, Waltham, MA, USA) using SDS software. Relative gene expression was calculated using the comparative cycle threshold (Ct) value method as previously described [73]. Results were normalized to Glyceraldehyde 3-phosphate dehydrogenase (GAPDH) and expressed relative to WJ-MSCs' gene expression.

#### 4.8. Statistical Analyses

All experiments and assays were done in technical duplicates or triplicates for three biological samples. Results were compounded and statistical significance was estimated with a two-tailed Student's *t*-test assuming equal variance performed in GraphPad Prism version 8.0. Data were presented as mean  $\pm$  standard error of the mean (SEM) as previously described [73].

**Supplementary Materials:** The following are available online at <http://www.mdpi.com/1422-0067/21/17/6437/s1>, Table S1: Antibodies used in the study, Table S2: Primers used in the study.

**Author Contributions:** A.A.M., H.A., M.A. and F.A.-M. conceived the study design. A.A.M., H.A., S.S. and F.A.-M. were involved in data acquisition, data analysis, and interpretation. A.A.M. performed the cell cultures, RNA, and protein extracts. S.K.M. and D.H. performed the Western blots assays. M.M. performed RT-PCR assays. M.A.-F. performed the Mass Spectrometry assays. A.A.M. wrote and S.S. edited the manuscript. All authors contributed to the drafting and critical review of the manuscript. All authors have read and agreed to the published version of the manuscript.

**Funding:** This work was funded by Kuwait Foundation for the Advancement of Sciences (KFAS) under project number RA-2013-009.

**Acknowledgments:** The authors would like to thank the Kuwait Foundation for the Advancement of Sciences (KFAS) and the Dasman Diabetes Institute for financial support. The authors would also like to thank Diana Marouco for helping to write and edit the manuscript.

**Conflicts of Interest:** The authors declare no conflict of interest.

## Abbreviations

ASFs	Adult skin fibroblasts
MS	Mass spectrometry
MSCs	Mesenchymal stem cells
NFFs	Neonate foreskin fibroblasts
WJ-MSCs	Wharton’s jelly-derived mesenchymal stem cells
Nano LC-MS/MS	Nanoscale liquid chromatography coupled to tandem mass spectrometry
GO	Gene ontology
EphA2	Ephrin type-A receptor 2
TLN2	Talin 2
CDH2	Cadherin-2 or N-cadherin
VDAC-3	Voltage-dependent anion-selective channel protein-3
SOD-2	Superoxide dismutase-2
ITGA-2	Integrin alpha subunit-2
LMF-2	Lipase maturation factor-2
SLC25A4	Solute Carrier Family 25 Member 4
PLEC1	Plectin-1
MLCK1	Myosin light chain kinase-1
ANTs	Adenine nucleotide translocases
HPA	Human protein atlas
qRT-PCR	Real-time quantitative reverse transcription polymerase chain reaction

## References

1. Ali, H.; Al-Yatama, M.K.; Abu-Farha, M.; Behbehani, K.; Al Madhoun, A. Multi-lineage differentiation of human umbilical cord Wharton’s Jelly Mesenchymal Stromal Cells mediates changes in the expression profile of stemness markers. *PLoS ONE* **2015**, *10*, e0122465. [[CrossRef](#)] [[PubMed](#)]
2. Alt, E.; Yan, Y.; Gehmert, S.; Song, Y.H.; Altman, A.; Gehmert, S.; Vykoukal, D.; Bai, X. Fibroblasts share mesenchymal phenotypes with stem cells, but lack their differentiation and colony-forming potential. *Biol. Cell* **2011**, *103*, 197–208. [[CrossRef](#)] [[PubMed](#)]
3. Gneccchi, M.; Zhang, Z.; Ni, A.; Dzau, V.J. Paracrine mechanisms in adult stem cell signaling and therapy. *Circ. Res.* **2008**, *103*, 1204–1219. [[CrossRef](#)] [[PubMed](#)]
4. Friedenstein, A.J.; Piatetzky-Shapiro, I.I.; Petrakova, K.V. Osteogenesis in transplants of bone marrow cells. *J. Embryol. Exp. Morphol.* **1966**, *16*, 381–390. [[PubMed](#)]
5. Zuk, P.A.; Zhu, M.; Mizuno, H.; Huang, J.; Futrell, J.W.; Katz, A.J.; Benhaim, P.; Lorenz, H.P.; Hedrick, M.H. Multilineage cells from human adipose tissue: Implications for cell-based therapies. *Tissue Eng.* **2001**, *7*, 211–228. [[CrossRef](#)] [[PubMed](#)]
6. Atari, M.; Barajas, M.; Hernandez-Alfaro, F.; Gil, C.; Fabregat, M.; Ferres Padro, E.; Giner, L.; Casals, N. Isolation of pluripotent stem cells from human third molar dental pulp. *Histol. Histopathol.* **2011**, *26*, 1057–1070. [[PubMed](#)]
7. Berebichez-Fridman, R.; Montero-Olvera, P.R. Sources and Clinical Applications of Mesenchymal Stem Cells: State-of-the-art review. *Sultan Qaboos Univ. Med. J.* **2018**, *18*, e264–e277. [[CrossRef](#)]
8. Cheng, H.Y.; Ghetu, N.; Huang, W.C.; Wang, Y.L.; Wallace, C.G.; Wen, C.J.; Chen, H.C.; Shih, L.Y.; Lin, C.F.; Hwang, S.M.; et al. Syngeneic adipose-derived stem cells with short-term immunosuppression induce vascularized composite allotransplantation tolerance in rats. *Cytotherapy* **2014**, *16*, 369–380. [[CrossRef](#)]
9. Mueller, S.M.; Glowacki, J. Age-related decline in the osteogenic potential of human bone marrow cells cultured in three-dimensional collagen sponges. *J. Cell Biochem.* **2001**, *82*, 583–590. [[CrossRef](#)]
10. Choudhery, M.S.; Badowski, M.; Muise, A.; Pierce, J.; Harris, D.T. Donor age negatively impacts adipose tissue-derived mesenchymal stem cell expansion and differentiation. *J. Transl. Med.* **2014**, *12*, 8. [[CrossRef](#)]
11. Dominici, M.; Le Blanc, K.; Mueller, L.; Slaper-Cortenbach, I.; Marini, F.C.; Krause, D.S.; Deans, R.J.; Keating, A.; Prockop, D.J.; Horwitz, E.M. Minimal criteria for defining multipotent mesenchymal stromal cells. The International Society for Cellular Therapy position statement. *Cytotherapy* **2006**, *8*, 315–317. [[CrossRef](#)] [[PubMed](#)]

12. Ali, H.; Al-Mulla, F. Defining umbilical cord blood stem cells. *Stem Cell Discov.* **2012**, *2*, 15–23. [[CrossRef](#)]
13. Joerger-Messerli, M.S.; Marx, C.; Oppliger, B.; Mueller, M.; Surbek, D.V.; Schoeberlein, A. Mesenchymal Stem Cells from Wharton's Jelly and Amniotic Fluid. *Best Pract. Res. Clin. Obstet. Gynaecol.* **2016**, *31*, 30–44. [[CrossRef](#)] [[PubMed](#)]
14. Wang, H.S.; Hung, S.C.; Peng, S.T.; Huang, C.C.; Wei, H.M.; Guo, Y.J.; Fu, Y.S.; Lai, M.C.; Chen, C.C. Mesenchymal stem cells in the Wharton's jelly of the human umbilical cord. *Stem Cells* **2004**, *22*, 1307–1330. [[CrossRef](#)] [[PubMed](#)]
15. Bagher, Z.; Azami, M.; Ebrahimi-Barough, S.; Mirzadeh, H.; Solouk, A.; Soleimani, M.; Ai, J.; Nourani, M.R.; Joghataei, M.T. Differentiation of Wharton's Jelly-Derived Mesenchymal Stem Cells into Motor Neuron-Like Cells on Three-Dimensional Collagen-Grafted Nanofibers. *Mol. Neurobiol.* **2016**, *53*, 2397–2408. [[CrossRef](#)]
16. Weiss, M.L.; Anderson, C.; Medicetty, S.; Seshareddy, K.B.; Weiss, R.J.; Vanderwerff, I.; Troyer, D.; McIntosh, K.R. Immune Properties of Human Umbilical Cord Wharton's Jelly-Derived Cells. *Stem Cells* **2008**, *26*, 2865–2874. [[CrossRef](#)]
17. Al Madhoun, A.; Alkandari, S.; Ali, H.; Carrio, N.; Atari, M.; Bitar, M.S.; Al-Mulla, F. Chemically Defined Conditions Mediate an Efficient Induction of Mesodermal Lineage from Human Umbilical Cord- and Bone Marrow- Mesenchymal Stem Cells and Dental Pulp Pluripotent-Like Stem Cells. *Cell Reprogram.* **2018**, *20*, 9–16. [[CrossRef](#)]
18. Al Madhoun, A.; Ali, H.; AlKandari, S.; Atizado, V.L.; Akhter, N.; Al-Mulla, F.; Atari, M. Defined three-dimensional culture conditions mediate efficient induction of definitive endoderm lineage from human umbilical cord Wharton's jelly mesenchymal stem cells. *Stem Cell Res. Ther.* **2016**, *7*, 165. [[CrossRef](#)]
19. Liang, J.; Wu, S.; Zhao, H.; Li, S.L.; Liu, Z.X.; Wu, J.; Zhou, L. Human umbilical cord mesenchymal stem cells derived from Wharton's jelly differentiate into cholinergic-like neurons in vitro. *Neurosci. Lett.* **2013**, *532*, 59–63. [[CrossRef](#)]
20. Bhandari, D.R.; Seo, K.W.; Sun, B.; Seo, M.S.; Kim, H.S.; Seo, Y.J.; Marcin, J.; Forraz, N.; Roy, H.L.; Larry, D.; et al. The simplest method for in vitro beta-cell production from human adult stem cells. *Differentiation* **2011**, *82*, 144–152. [[CrossRef](#)]
21. Stern-Straeter, J.; Bonaterra, G.A.; Juritz, S.; Birk, R.; Goessler, U.R.; Bieback, K.; Bugert, P.; Schultz, J.; Hormann, K.; Kinscherf, R.; et al. Evaluation of the effects of different culture media on the myogenic differentiation potential of adipose tissue- or bone marrow-derived human mesenchymal stem cells. *Int. J. Mol. Med.* **2014**, *33*, 160–170. [[CrossRef](#)] [[PubMed](#)]
22. Balasubramanian, S.; Thej, C.; Venugopal, P.; Priya, N.; Zakaria, Z.; Sundarraj, S.; Majumdar, A.S. Higher propensity of Wharton's jelly derived mesenchymal stromal cells towards neuronal lineage in comparison to those derived from adipose and bone marrow. *Cell Biol. Int.* **2013**, *37*, 507–515. [[CrossRef](#)] [[PubMed](#)]
23. Yang, J.; Song, T.; Wu, P.; Chen, Y.; Fan, X.; Chen, H.; Zhang, J.; Huang, C. Differentiation potential of human mesenchymal stem cells derived from adipose tissue and bone marrow to sinus node-like cells. *Mol. Med. Rep.* **2012**, *5*, 108–113.
24. Meligy, F.Y.; Shigemura, K.; Behnsawy, H.M.; Fujisawa, M.; Kawabata, M.; Shirakawa, T. The efficiency of in vitro isolation and myogenic differentiation of MSCs derived from adipose connective tissue, bone marrow, and skeletal muscle tissue. *Vitro Cell Dev. Biol. Anim.* **2012**, *48*, 203–215. [[CrossRef](#)] [[PubMed](#)]
25. Gauthaman, K.; Fong, C.Y.; Suganya, C.A.; Subramanian, A.; Biswas, A.; Choolani, M.; Bongso, A. Extra-embryonic human Wharton's jelly stem cells do not induce tumorigenesis, unlike human embryonic stem cells. *Reprod. Biomed. Online* **2012**, *24*, 235–246. [[CrossRef](#)] [[PubMed](#)]
26. Zeddou, M.; Briquet, A.; Relic, B.; Josse, C.; Malaise, M.G.; Gothot, A.; Lechanteur, C.; Beguin, Y. The umbilical cord matrix is a better source of mesenchymal stem cells (MSC) than the umbilical cord blood. *Cell Biol. Int.* **2010**, *34*, 693–701. [[CrossRef](#)]
27. Fong, C.Y.; Chak, L.L.; Biswas, A.; Tan, J.H.; Gauthaman, K.; Chan, W.K.; Bongso, A. Human Wharton's jelly stem cells have unique transcriptome profiles compared to human embryonic stem cells and other mesenchymal stem cells. *Stem Cell Rev.* **2011**, *7*, 1–16. [[CrossRef](#)]
28. Hsieh, J.Y.; Fu, Y.S.; Chang, S.J.; Tsuang, Y.H.; Wang, H.W. Functional module analysis reveals differential osteogenic and stemness potentials in human mesenchymal stem cells from bone marrow and Wharton's jelly of umbilical cord. *Stem. Cells Dev.* **2010**, *19*, 1895–1910. [[CrossRef](#)]
29. Jiang, W.; Xu, J. Immune modulation by mesenchymal stem cells. *Cell Prolif.* **2020**, *53*, e12712. [[CrossRef](#)]

30. Abumaree, M.; Al Jumah, M.; Pace, R.A.; Kalionis, B. Immunosuppressive properties of mesenchymal stem cells. *Stem Cell Rev. Rep.* **2012**, *8*, 375–392. [[CrossRef](#)]
31. Melief, S.M.; Geutskens, S.B.; Fibbe, W.E.; Roelofs, H. Multipotent stromal cells skew monocytes towards an anti-inflammatory function: The link with key immunoregulatory molecules. *Haematologica* **2013**, *98*, e121–e122. [[CrossRef](#)] [[PubMed](#)]
32. Spaggiari, G.M.; Capobianco, A.; Abdelrazik, H.; Becchetti, F.; Mingari, M.C.; Moretta, L. Mesenchymal stem cells inhibit natural killer-cell proliferation, cytotoxicity, and cytokine production: Role of indoleamine 2,3-dioxygenase and prostaglandin E2. *Blood* **2008**, *111*, 1327–1333. [[CrossRef](#)] [[PubMed](#)]
33. Obermayer, N.; Popp, F.C.; Soeder, Y.; Haarer, J.; Geissler, E.K.; Schlitt, H.J.; Dahlke, M. H Conversion of Th17 into IL-17A(neg) regulatory T cells: A novel mechanism in prolonged allograft survival promoted by mesenchymal stem cell-supported minimized immunosuppressive therapy. *J. Immunol.* **2014**, *193*, 4988–4999. [[CrossRef](#)] [[PubMed](#)]
34. Yoo, K.H.; Jang, I.K.; Lee, M.W.; Kim, H.E.; Yang, M.S.; Eom, Y.; Lee, J.E.; Kim, Y.J.; Yang, S.K.; Jung, H.L.; et al. Comparison of immunomodulatory properties of mesenchymal stem cells derived from adult human tissues. *Cell Immunol.* **2009**, *259*, 150–156. [[CrossRef](#)]
35. Valencia, J.; Blanco, B.; Yanez, R.; Vazquez, M.; Herrero Sanchez, C.; Fernandez-Garcia, M.; Rodriguez Serrano, C.; Pescador, D.; Blanco, J.F.; Hernando-Rodriguez, M.; et al. Comparative analysis of the immunomodulatory capacities of human bone marrow- and adipose tissue-derived mesenchymal stromal cells from the same donor. *Cytotherapy* **2016**, *18*, 1297–1311. [[CrossRef](#)]
36. Melief, S.M.; Zwaginga, J.J.; Fibbe, W.E.; Roelofs, H. Adipose tissue-derived multipotent stromal cells have a higher immunomodulatory capacity than their bone marrow-derived counterparts. *Stem Cells Transl. Med.* **2013**, *2*, 455–463. [[CrossRef](#)]
37. Petrenko, Y.; Vackova, I.; Kekulova, K.; Chudickova, M.; Koci, Z.; Turnovcova, K.; Kupcova Skalnikova, H.; Vodicka, P.; Kubinova, S. A Comparative Analysis of Multipotent Mesenchymal Stromal Cells derived from Different Sources, with a Focus on Neuroregenerative Potential. *Sci. Rep.* **2020**, *10*, 4290. [[CrossRef](#)]
38. Ribeiro, A.; Laranjeira, P.; Mendes, S.; Velada, I.; Leite, C.; Andrade, P.; Santos, F.; Henriques, A.; Graos, M.; Cardoso, C.M.; et al. Mesenchymal stem cells from umbilical cord matrix, adipose tissue and bone marrow exhibit different capability to suppress peripheral blood B, natural killer and T cells. *Stem Cell Res.* **2013**, *4*, 125. [[CrossRef](#)]
39. Kalaszczynska, I.; Ferdyn, K. Wharton’s jelly derived mesenchymal stem cells: Future of regenerative medicine? Recent findings and clinical significance. *Biomed Res. Int.* **2015**, *2015*, 430847. [[CrossRef](#)]
40. Wang, Q.; Yang, Q.; Wang, Z.; Tong, H.; Ma, L.; Zhang, Y.; Shan, F.; Meng, Y.; Yuan, Z. Comparative analysis of human mesenchymal stem cells from fetal-bone marrow, adipose tissue, and Warton’s jelly as sources of cell immunomodulatory therapy. *Hum. Vaccin. Immunother.* **2016**, *12*, 85–96. [[CrossRef](#)]
41. Kendall, R.T.; Feghali-Bostwick, C. A Fibroblasts in fibrosis: Novel roles and mediators. *Front. Pharmacol.* **2014**, *5*, 123. [[CrossRef](#)] [[PubMed](#)]
42. Halfon, S.; Abramov, N.; Grinblat, B.; Ginis, I. Markers distinguishing mesenchymal stem cells from fibroblasts are downregulated with passaging. *Stem Cells Dev.* **2011**, *20*, 53–66. [[CrossRef](#)] [[PubMed](#)]
43. De Sousa Abreu, R.; Penalva, L.O.; Marcotte, E.M.; Vogel, C. Global signatures of protein and mRNA expression levels. *Mol. Biosyst.* **2009**, *5*, 1512–1526. [[CrossRef](#)]
44. Brohem, C.A.; de Carvalho, C.M.; Radoski, C.L.; Santi, F.C.; Baptista, M.C.; Swinka, B.B.; de A. Urban, C.; de Araujo, L.R.; Graf, R.M.; Feferman, I.H.; et al. Comparison between fibroblasts and mesenchymal stem cells derived from dermal and adipose tissue. *Int. J. Cosmet. Sci.* **2013**, *35*, 448–457. [[CrossRef](#)]
45. Denu, R.A.; Nemcek, S.; Bloom, D.D.; Goodrich, A.D.; Kim, J.; Mosher, D.F.; Hematti, P. Fibroblasts and Mesenchymal Stromal/Stem Cells Are Phenotypically Indistinguishable. *Acta Haematol.* **2016**, *136*, 85–97. [[CrossRef](#)] [[PubMed](#)]
46. Lorenz, K.; Sicker, M.; Schmelzer, E.; Rupf, T.; Salvetter, J.; Schulz-Siegmund, M.; Bader, A. Multilineage differentiation potential of human dermal skin-derived fibroblasts. *Exp. Dermatol.* **2008**, *17*, 925–932. [[CrossRef](#)] [[PubMed](#)]
47. Sudo, K.; Kanno, M.; Miharada, K.; Ogawa, S.; Hiroyama, T.; Saijo, K.; Nakamura, Y. Mesenchymal progenitors able to differentiate into osteogenic, chondrogenic, and/or adipogenic cells in vitro are present in most primary fibroblast-like cell populations. *Stem Cells* **2007**, *25*, 1610–1617. [[CrossRef](#)]

48. Alfaro, D.; Zapata, A.G. Eph/Ephrin-mediated stimulation of human bone marrow mesenchymal stromal cells correlates with changes in cell adherence and increased cell death. *Stem Cell Res.* **2018**, *9*, 172. [[CrossRef](#)] [[PubMed](#)]
49. Taylor, H.; Campbell, J.; Nobes, C.D. Ephs and ephrins. *Curr. Biol.* **2017**, *27*, R90–R95. [[CrossRef](#)]
50. Goldshmit, Y.; McLenachan, S.; Turnley, A. Roles of Eph receptors and ephrins in the normal and damaged adult CNS. *Brain Res. Rev.* **2006**, *52*, 327–345. [[CrossRef](#)]
51. Binda, E.; Visioli, A.; Giani, F.; Lamorte, G.; Copetti, M.; Pitter, K.L.; Huse, J.T.; Cajola, L.; Zanetti, N.; DiMeco, F.; et al. The EphA2 receptor drives self-renewal and tumorigenicity in stem-like tumor-propagating cells from human glioblastomas. *Cancer Cell* **2012**, *22*, 765–780. [[CrossRef](#)] [[PubMed](#)]
52. Jung, Y.H.; Lee, S.J.; Oh, S.Y.; Lee, H.J.; Ryu, J.M.; Han, H.J. Oleic acid enhances the motility of umbilical cord blood derived mesenchymal stem cells through EphB2-dependent F-actin formation. *Biochim. Biophys. Acta* **2015**, *1853*, 1905–1917. [[CrossRef](#)] [[PubMed](#)]
53. Shen, S.P.; Liu, W.T.; Lin, Y.; Li, Y.T.; Chang, C.H.; Chang, F.W.; Wang, L.M.; Teng, S.W.; Hsuan, Y. EphA2 is a biomarker of hMSCs derived from human placenta and umbilical cord. *Taiwan J. Obs. Gynecol.* **2015**, *54*, 749–756. [[CrossRef](#)] [[PubMed](#)]
54. Wen, Y.C.; Du, M.K.; Li, M.W.; Hsuan, Y.C.; Su, Y.C.; Lin, W. EphA2-positive human umbilical cord-derived mesenchymal stem cells exert anti-fibrosis and immunomodulatory activities via secretion of prostaglandin E2. *Taiwan J. Obs. Gynecol.* **2018**, *57*, 722–725. [[CrossRef](#)]
55. Toran, J.L.; Lopez, J.A.; Gomes-Alves, P.; Aguilar, S.; Torroja, C.; Trevisan-Herraz, M.; Moscoso, I.; Sebastiao, M.J.; Serra, M.; Brito, C.; et al. Definition of a cell surface signature for human cardiac progenitor cells after comprehensive comparative transcriptomic and proteomic characterization. *Sci. Rep.* **2019**, *9*, 4647. [[CrossRef](#)]
56. Choi, M.; Lee, H.S.; Naidansaren, P.; Kim, H.K.; O, E.; Cha, J.H.; Ahn, H.Y.; Yang, P.I.; Shin, J.C.; Joe, Y.A. Proangiogenic features of Wharton’s jelly-derived mesenchymal stromal/stem cells and their ability to form functional vessels. *Int. J. Biochem. Cell Biol.* **2013**, *45*, 560–570. [[CrossRef](#)]
57. Dejana, E.; Orsenigo, F.; Molendini, C.; Baluk, P.; McDonald, D.M. Organization and signaling of endothelial cell-to-cell junctions in various regions of the blood and lymphatic vascular trees. *Cell Tissue. Res.* **2009**, *335*, 17–25. [[CrossRef](#)]
58. Yoo, J.K.; Kim, J.; Choi, S.J.; Noh, H.M.; Kwon, Y.D.; Yoo, H.; Yi, H.S.; Chung, H.M.; Kim, J.K. Discovery and characterization of novel microRNAs during endothelial differentiation of human embryonic stem cells. *Stem Cells Dev.* **2012**, *21*, 2049–2057. [[CrossRef](#)]
59. Adorno-Cruz, V.; Liu, H. Regulation and functions of integrin alpha2 in cell adhesion and disease. *Genes Dis.* **2019**, *6*, 16–24. [[CrossRef](#)]
60. Ginsberg, M.H. Integrin activation. *BMB Rep.* **2014**, *47*, 655–659. [[CrossRef](#)]
61. Ye, F.; Snider, A.K.; Ginsberg, M.H.; Ye, F.; Snider, A.K.; Ginsberg, M.H. Talin and kindlin: The one-two punch in integrin activation. *Front Med.* **2014**, *8*, 6–16. [[CrossRef](#)] [[PubMed](#)]
62. Cappellesso-Fleury, S.; Puissant-Lubrano, B.; Apoil, P.A.; Titeux, M.; Winterton, P.; Casteilla, L.; Bourin, P.; Blancher, A. Human fibroblasts share immunosuppressive properties with bone marrow mesenchymal stem cells. *J. Clin. Immunol.* **2010**, *30*, 607–619. [[CrossRef](#)] [[PubMed](#)]
63. Uhlen, M.; Fagerberg, L.; Hallstrom, B.M.; Lindskog, C.; Oksvold, P.; Mardinoglu, A.; Sivertsson, A.; Kampf, C.; Sjostedt, E.; Asplund, A.; et al. Proteomics. Tissue-based map of the human proteome. *Science* **2015**, *347*, 1260419. [[CrossRef](#)]
64. Thul, P.J.; Akesson, L.; Wiking, M.; Mahdessian, D.; Geladaki, A.; Ait Blal, H.; Alm, T.; Asplund, A.; Bjork, L.; Breckels, L.M.; et al. A subcellular map of the human proteome. *Science* **2017**, *356*. [[CrossRef](#)] [[PubMed](#)]
65. Mafi, P.; Hindocha, S.; Mafi, R.; Griffin, M.; Khan, W.S. Adult mesenchymal stem cells and cell surface characterization—A systematic review of the literature. *Open Orthop. J.* **2011**, *5*, 253–260. [[CrossRef](#)] [[PubMed](#)]
66. Zhou, H.; Wang, F.; Wang, Y.; Ning, Z.; Hou, W.; Wright, T.G.; Sundaram, M.; Zhong, S.; Yao, Z.; Figeys, D. Improved recovery and identification of membrane proteins from rat hepatic cells using a centrifugal proteomic reactor. *Mol. Cell Proteomics* **2011**, *10*, O111 008425. [[CrossRef](#)]
67. Abu-Farha, M.; Tiss, A.; Abubaker, J.; Khadir, A.; Al-Ghimlas, F.; Al-Khairi, I.; Baturcam, E.; Cherian, P.; Elkum, N.; Hammad, M.; et al. Proteomics analysis of human obesity reveals the epigenetic factor HDAC4 as a potential target for obesity. *PLoS ONE* **2013**, *8*, e75342. [[CrossRef](#)] [[PubMed](#)]

68. Al Madhoun, A.S.; Mehta, V.; Li, G.; Figeys, D.; Wiper-Bergeron, N.; Skerjanc, I. Skeletal myosin light chain kinase regulates skeletal myogenesis by phosphorylation of MEF2C. *EMBO J.* **2011**, *30*, 2477–2489. [[CrossRef](#)]
69. Voronova, A.; Al Madhoun, A.; Fischer, A.; Shelton, M.; Karamboulas, C.; Skerjanc, I.S. Gli2 and MEF2C activate each other's expression and function synergistically during cardiomyogenesis in vitro. *Nucleic Acids Res.* **2012**, *40*, 3329–3347. [[CrossRef](#)]
70. Khadir, A.; Tiss, A.; Abubaker, J.; Abu-Farha, M.; Al-Khairi, I.; Cherian, P.; John, J.; Kavalakatt, S.; Warsame, S.; Al-Madhoun, A.; et al. MAP kinase phosphatase DUSP1 is overexpressed in obese humans and modulated by physical exercise. *Am. J. Physiol. Endocrinol. Metab.* **2015**, *308*, E71–E83. [[CrossRef](#)]
71. Al-Madhoun, A.S.; van der Wilt, C.L.; Loves, W.J.; Padron, J.M.; Eriksson, S.; Talianidis, I.; Peters, G.J. Detection of an alternatively spliced form of deoxycytidine kinase mRNA in the 2'-2'-difluorodeoxycytidine (gemcitabine)-resistant human ovarian cancer cell line AG6000. *Biochem. Pharmacol.* **2004**, *68*, 601–609. [[CrossRef](#)] [[PubMed](#)]
72. Wang, X.W.; Seed, B. A PCR primer bank for quantitative gene expression analysis. *Nucleic Acids Res.* **2003**, *31*, e154. [[CrossRef](#)] [[PubMed](#)]
73. Al Madhoun, A.S.; Voronova, A.; Ryan, T.; Zakariyah, A.; McIntire, C.; Gibson, L.; Shelton, M.; Ruel, M.; Skerjanc, I.S. Testosterone enhances cardiomyogenesis in stem cells and recruits the androgen receptor to the MEF2C and HCN4 genes. *J. Mol. Cell Cardiol.* **2013**, *60*, 164–171. [[CrossRef](#)] [[PubMed](#)]



© 2020 by the authors. Licensee MDPI, Basel, Switzerland. This article is an open access article distributed under the terms and conditions of the Creative Commons Attribution (CC BY) license (<http://creativecommons.org/licenses/by/4.0/>).